

Article

A Merging Approach for Improving the Quality of Gridded Precipitation Datasets over Burkina Faso

Moussa Waongo ^{1,*}, Juste Nabassebeguelogo Garba ², Ulrich Jacques Diasso ², Windmanagda Sawadogo ³,
Wendyam Lazare Sawadogo ² and Tizane Daho ⁴

¹ AGRHYMET Regional Centre, Niamey BP 11011, Niger

² Agence Nationale de La Meteorologie (ANAM), Ouagadougou BP 576, Burkina Faso; garba.juste@meteoburkina.bf (J.N.G.); diassou@africa-union.org (U.J.D.); sawadogo.lazare@meteoburkina.bf (W.L.S.)

³ Institute of Geography, University of Augsburg, 86159 Augsburg, Germany; windmanagda.sawadogo@geo.uni-augsburg.de

⁴ Laboratory of Environmental Physics and Chemistry, Joseph KI-ZERBO University, Ouagadougou BP 7021, Burkina Faso; tizane.daho@ujkz.bf

* Correspondence: moussa.waongo@cilss.int

Abstract: Satellite precipitation estimates are crucial for managing climate-related risks such as droughts and floods. However, these datasets often contain systematic errors due to the observation methods used. The accuracy of these estimates can be enhanced by integrating spatial and temporal resolution data from in situ observations. Nevertheless, the accuracy of the merged dataset is influenced by the density and distribution of rain gauges, which can vary regionally. This paper presents an approach to improve satellite precipitation data (SPD) over Burkina Faso. Two bias correction methods, Empirical Quantile Mapping (EQM) and Time and Space-Variant (TSV), have been applied to the SPD to yield a bias-corrected dataset for the period 1991–2020. The most accurate bias-corrected dataset is then combined with in situ observations using the Regression Kriging (RK) method to produce a merged precipitation dataset. The findings show that both bias correction methods achieve similar reductions in RMS error, with higher correlation coefficients (approximately 0.8–0.9) and a normalized standard deviation closer to 1. However, EQM generally demonstrates more robust and consistent performance, particularly in terms of correlation and RMS error reduction. On a monthly scale, the superiority of EQM is most evident in June, September, and October. Following the merging process, the final dataset, which incorporates satellite information in addition to in situ observations, demonstrates higher performance. It shows improvements in the coefficient of determination by 83%, bias by 11.4%, mean error by 96.7%, and root-mean-square error by 95.5%. The operational implementation of this approach provides substantial support for decision-making in regions heavily reliant on rainfed agriculture and sensitive to climate variability. Delivering more precise and reliable precipitation datasets enables more informed decisions and significantly enhances policy-making processes in the agricultural and water resources sectors of Burkina Faso.

Keywords: gauge precipitation; TAMSAT estimates; merging approach; Empirical Quantile Mapping; Regression Kriging; Burkina Faso



Citation: Waongo, M.; Garba, J.N.; Diasso, U.J.; Sawadogo, W.; Sawadogo, W.L.; Daho, T. A Merging Approach for Improving the Quality of Gridded Precipitation Datasets over Burkina Faso. *Climate* **2024**, *12*, 226. <https://doi.org/10.3390/cli12120226>

Received: 11 November 2024

Revised: 15 December 2024

Accepted: 17 December 2024

Published: 20 December 2024



Copyright: © 2024 by the authors. Licensee MDPI, Basel, Switzerland. This article is an open access article distributed under the terms and conditions of the Creative Commons Attribution (CC BY) license (<https://creativecommons.org/licenses/by/4.0/>).

1. Introduction

Rainfall in West Africa, especially in the Sahel region, plays a fundamental role in shaping agricultural practices, water resource management, and food security. The Sahel, characterized by its semi-arid conditions, depends significantly on the rainy season to support agricultural productivity and the livelihoods of people [1,2]. Therefore, fluctuations in precipitation patterns can have severe impacts on agriculture. Indeed, the agricultural calendar is predominantly dictated by the seasonal distribution of precipitation. The types of crops that can be cultivated, their planting times, and harvest periods are influenced

by water availability [3]. Hence, the variability and change in precipitation patterns can lead to crop failures, reduce food availability, and pose significant risks to food security in West Africa. In this context, timely and accurate precipitation forecasts are vital to enable farmers to adjust their practices in response to predicted changes in precipitation [4]. Despite its importance, obtaining accurate and high-resolution precipitation data remains challenging, particularly in regions with a sparse and unevenly distributed ground-based observation network. Indeed, the decline in rain gauge observations and inconsistent reporting across West Africa creates temporal inconsistencies and sampling errors in rainfall data [5]. To address these challenges, satellite precipitation estimates are often used to improve coverage. However, these data often suffer from biases and errors due to the indirect nature of the measurements.

Satellite estimates are subject to random error, which is inherent in measurement records, and systematic bias related to post-processing algorithms and procedures [6,7]. As described by [8], this systematic difference between satellite and terrestrial observations is known as bias. The bias is highly dependent on the location, topography, season, and hydroclimatic characteristics of the study area [9]. Thus, satellite datasets must be adjusted before being used as input data for impact study models or other applications [10]. Several bias correction techniques have been developed in an attempt to improve satellite precipitation datasets (SPDs) and are discussed in detail in numerous publications [11–14]. Each bias correction approach has its strengths and weaknesses. Indeed, the literature suggests that while bias correction methods can be tailored for specific uses, achieving a universally superior method is challenged by the inherent complexities and contextual dependencies of bias characteristics. Thus, the ongoing assessment and development of bias correction methodologies remain essential to address specific analytical requirements efficiently [15]. Therefore, attempts at evaluating the performance of different bias correction methods have not yielded a universal best bias correction technique [16]. However, some studies reported that the distribution-based approach has been more successful in reproducing precipitation than both linear and non-linear approaches. Among these methods, Empirical Quantile Mapping (EQM) reveals higher performance, remains the most widely used bias correction, and is also known to be the most effective. For instance, an evaluation of various bias correction methods in climate models highlighted EQM's effectiveness in reducing biases, particularly for frequency-based indices and seasonal mean precipitation, showing its robustness in different climatic conditions [17]. However, this approach is highly sensitive to calibration periods, highlighting the importance of careful methodological application to ensure successful outcomes [18]. Among the dynamic methods, the Time and Space Variant (TSV) performed better in the majority of evaluation studies [16,19]. TSV enhancement is recognized for its capacity to significantly improve the spatial accuracy of precipitation measurements [20]. Although the bias correction process improves satellite-derived data accuracy, merging satellite data with rain gauge data leverages the spatial coverage of satellites and the point accuracy of rain gauges, thereby producing a dataset that is superior to either source alone.

Previous studies have shown that merging approaches have many advantages [21,22]. They integrate the spatial coverage of satellite data with the ground-based high temporal measurements and improve the temporal consistency, thereby ensuring that the merged dataset accurately reflects local precipitation patterns. Among various merging techniques, Regression Kriging (RK) stands out as a particularly effective method for combining satellite and gauge data in regions with uneven rain gauge distribution [23,24]. RK's strength lies in its hybrid approach that combines deterministic regression modeling with geostatistical interpolation, allowing it to capture both large-scale trends and local spatial variations in precipitation patterns [25,26]. This dual approach is especially valuable in the Sahel region, where precipitation patterns show strong spatial heterogeneity and where rain gauge networks are sparse and unevenly distributed [5]. Indeed, the accuracy of the merged dataset can be limited by the density and distribution of rain gauges, which are regional or country-specific [27,28]. Moreover, while integrating ground-based precipitation measurements

with satellite data is advantageous, the specific method of incorporating gauge data can significantly impact the quality and accuracy of the final rainfall estimates [29].

In this regard, this study presents a merging approach aimed at accounting for the quality and availability of ground-based precipitation observations and the need for calibration and validation of satellite estimates against ground-based observation data in West Africa. Unlike many studies that merge satellite and gauge data directly, this approach first evaluates SPDs and applies bias correction techniques to reduce systematic errors before the merging process. Using Burkina Faso as a regional focus, this approach aims to provide accurate and high-resolution precipitation data for impact studies in West Africa, thereby supporting decision-making processes. This work is divided into four sections. Section 1 focuses on the study area, while Section 2 addresses data and methodology. The results are presented in Section 3, and Section 4 discusses these results, summarizes the key findings of this study, and offers some perspectives.

2. Materials and Methods

2.1. Study Area

Burkina Faso is a landlocked country in West Africa of more than 274,000 km² located in the tropical region within latitudes 9°20' and 15°05' north of the Equator and between longitudes 5°30' west and 2°20' east. The country is surrounded by six countries: Mali to the north and west; Niger to the east; Benin to the southeast; Togo to the southeast; Ghana to the south; and the Ivory Coast to the southwest. Burkina Faso has a tropical climate characterized by two seasons: wet and dry [30]. These seasons are influenced by the movement of two dominant winds: the rain-bearing southwesterly winds and the cold, dry, and dusty northeasterly winds, commonly known as the Harmattan period. Precipitation varies significantly, ranging from an average of 350 mm in the north to over 1000 mm in the southwest (Figure 1). The rainy season lasts an average of 5 months, from May to September, but its duration is shorter in the northern part of the country. Temperatures show great seasonal variations and diurnal amplitudes. Average temperatures are highest in March, April, and October and lowest in November, December, January, and February [31,32]. During the dry season, from December to May, the mean maximum temperatures range from 34 °C to 41 °C, while the mean minimum temperatures range from 16 °C to 26 °C. In contrast, during the rainy season, the diurnal temperature range decreases, and the mean maximum temperatures are approximately 30 °C to 36 °C, while the mean minimum temperatures vary between 20 °C and 25 °C [30].

2.2. Rain Gauge Measurements

Daily precipitation data from 140 rain gauges, covering the period from 1 January 1981 to 31 December 2023, were obtained from the National Meteorological Agency of Burkina Faso. From the precipitation dataset, quality control at the rain gauge station level was carried out to identify outliers, missing values, and inconsistent station coordinates. Stations with significant gaps (more than 5%) of data during the study period were excluded from the dataset. As a result, 97 stations were found to be reliable, with relatively consistent records for the period of 1991–2020. Figure 1 illustrates the location of the selected rain gauge stations, highlighting their uneven spatial distribution.

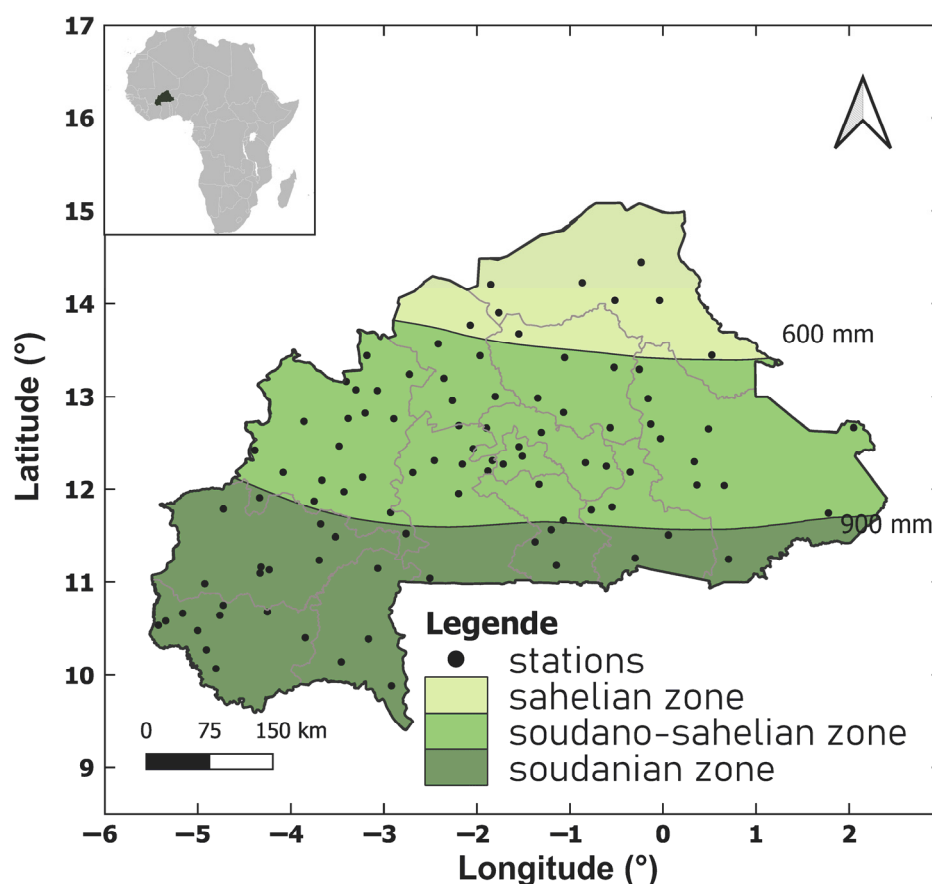


Figure 1. Spatial distribution of annual precipitation with rain gauge network in the study area.

2.3. Satellite Rainfall Estimates from TAMSAT

Precipitation data from version 3.1 of the satellite-based precipitation estimation system developed by the Tropical Applications of Meteorology using SATellite data and ground-based observations (TAMSAT) from the University of Reading in the UK were retrieved for merging purposes (available at <https://www.tamsat.org.uk> (accessed on 6 May 2024)). The TAMSAT approach for deriving precipitation data is based on identifying potentially rain-producing clouds by their cold temperatures at the top. This is achieved by deriving cloud top temperatures from METEOSAT thermal infrared (TIR) imagery provided by EUMETSAT. The time during which a pixel remains colder than a given temperature threshold is accumulated over 10-day (TAMSAT Version 2.0) or 5-day (TAMSAT Version 3.1) periods to create the Cold Cloud Duration (CCD) data. Rainfall estimates for periods of 10 days (dekadal) or 5 days (pentadal) are then calculated using a linear regression between ground-based observations of precipitation and CCD, as shown in Equation (1) [33].

$$pcp = a_0 + a_1 \times CDD \quad (1)$$

where pcp represents rainfall for a 10-day or 5-day period, and the parameters a_0 and a_1 are found through calibration using rain gauge data.

The performance of TAMSAT v3 compared to TAMSAT v2 is detailed in [34]. In addition, a former study by [35] indicated a good agreement in reproducing the precipitation pattern over Burkina Faso. Although TAMSAT benefited from worldwide data collection through the network of the Global Telecommunications System (GTS) of the World Meteorological Organization [36], ref. [5] pointed out that in West Africa, primarily synoptic stations report through the GTS network, which represents only a small fraction of the total rainfall monitoring network in the region. For instance, in Burkina Faso, the National Meteorological Agency operates only 10 synoptic stations out of 134 observation

stations [35], representing less than 10% of rain gauge data reported through the GTS. This limited data representation poses significant challenges for TAMSAT's ability to capture comprehensive rainfall patterns, suggesting that the integration of additional observational stations could substantially enhance the model's accuracy and utility for regional climate monitoring and forecasting applications.

2.4. Merging Approach

A merging approach algorithm is proposed for combining satellite precipitation datasets (SPDs) with in situ gauge precipitation data for Burkina Faso. The merging algorithm consists of three main steps: (1) quality control of rain gauge observations, (2) bias removal in the TAMSAT dataset based on rain gauge observations, and (3) merging the bias-corrected satellite dataset with the rain gauge observations to produce an improved quality daily dataset. The flowchart of the merging approach is presented in Figure 2.

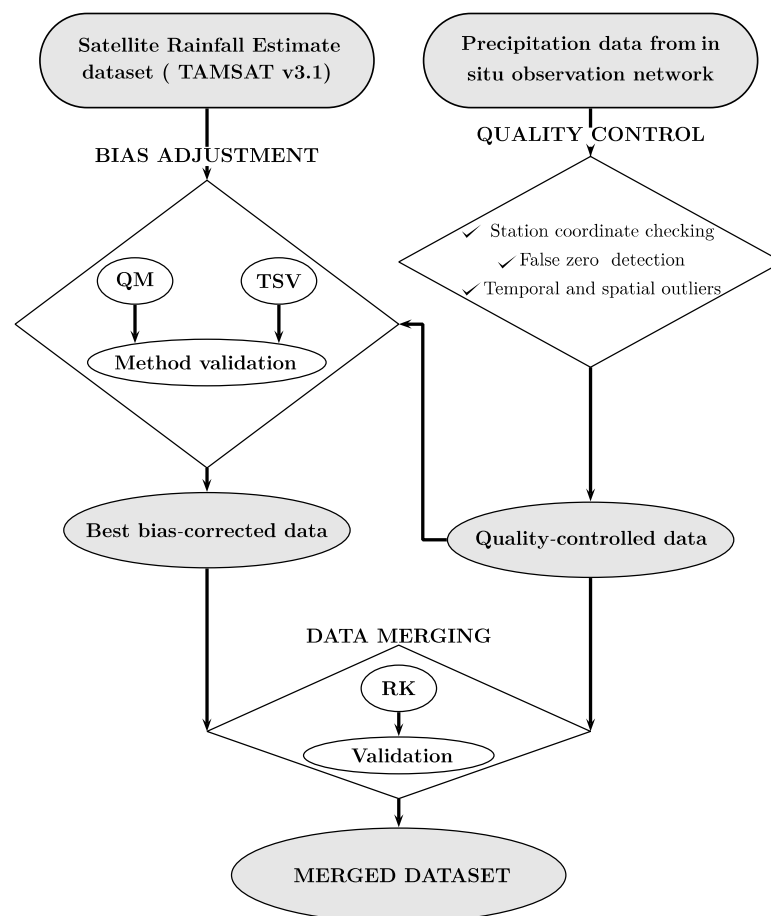


Figure 2. Flow chart describing the steps of the satellite–rain gauge data merging approach.

2.4.1. Quality Control

The availability of quality precipitation records in the current climate situation is of great importance in the merging process. However, many weather observation networks belonging to National Meteorological services do not always have reliable systems that guarantee the availability of long-term series of quality precipitation [37]. Errors can arise from various sources, such as a problem with the rain gauge, observer reading, data digitization, format conversion, or file manipulation and importation. In this study, a basic quality control consisting of detecting physically impossible or abnormal data [38,39]. The process encompasses the verification of the geographic coordinates of the stations, the detection of false zeros, and temporal and spatial outliers. Station coordinate checking allows for identifying duplicate and implausible coordinates, as well as stations located

outside of the study area. Verifying the geographic coordinates of the stations is important as the coordinates will later be used to extract satellite data [33]. Quality control was applied to the precipitation data obtained from the National Meteorological Agency of Burkina Faso.

Detection for false zeros involves checking for an incorrect report of zero precipitation during the rainy season for rainy season months. The source of false zeros is often ambiguity in the coding of days without observations (missing values) and days without precipitation (zero values) when digitizing paper records [33]. To check for false zeros, the percentage of zero values for each month at the target station is calculated and compared with the average percentage of zero values for the same month at neighboring stations.

Outlier checking has been performed by several authors as part of the station data quality control procedure [9,40,41]. A temporal check is conducted for each month to ensure that each observed value is consistent with the climatological data of the station [37]. Any suspect or aberrant values detected by this test are reported and must be carefully checked. A spatial check is performed by comparing each daily value of a given station with the values of neighboring stations recorded on the same date in order to verify whether the extreme values observed are the result of extreme climatic events [37]. Extremely high or low values, which differ significantly from the values recorded by neighboring stations, are set to missing values.

2.4.2. Bias Adjustment

Two bias correction schemes, namely Time and Space Variable (TSV) and Empirical Quantile Mapping (EQM), were applied to obtain bias-corrected daily precipitation time series at any point in the domain of interest [42]. Both methods are further evaluated to select the method that best corrects the TAMSAT data. Several studies demonstrated that TSV and EQM methods perform best in reproducing precipitation [35,43–45].

EQM is a distribution-based technique method that matches the cumulative distribution function (CDF) of the biased SPDs to the CDF of the rain gauge observations using a transfer function H . It uses the empirical nonparametric CDF without any assumptions about the precipitation distribution. For a given satellite precipitation value pcp_{sat} , the corrected precipitation pcp_{cor} can be expressed as Equation (2). As the most widely recognized and recent technique in bias correction of SPDs, QM has been implemented in several studies for the bias correction of regional climate models [43,46,47] and satellite precipitation estimates bias correction [6,10,48]. This method is used to correct the mean, standard deviation, and quantiles of SPDs to the mean, standard deviation, and quantiles of the rain gauge observations [6]. The transfer function, also called the correction function, is constructed to shift the distribution function of biased SPDs to the rain gauge distribution [42]. To implement the QM method, two empirical CDFs are calculated with historical precipitation. One CDF of biased SPDs and the second of the rain gauge observation for each day-of-the-year, in each observation station. The method for calculating empirical CDFs is described by [49]. The value of CDFs at each quantile is replaced by the CDF of the rain gauge observations, as illustrated in Figure 3 [12,50].

$$pcp_{cor} = H(pcp_{sat}) \quad (2)$$

$$H(pcp_{sat}) = CDF_{gauge}^{-1}[CDF_{sat}(pcp_{sat})]$$

$$CDF(pcp) = P(P \leq pcp) = \int_{-\infty}^{pcp} f(x)dx$$

$$CDF^{-1}(p) = \min x : P(X \leq x) \geq p$$

where pcp_{cor} is the corrected satellite precipitation, pcp_{sat} is the uncorrected satellite precipitation, $H(\cdot)$ is the transfer function, $CDF_{sat}(\cdot)$ is the Cumulative Distribution Function (CDF) of satellite precipitation, $CDF_{gauge}^{-1}(\cdot)$ is the inverse CDF of gauge precipitation, P is

the random variable representing precipitation, $f(x)$ is the probability density function of P , and p is a probability value in $[0,1]$.

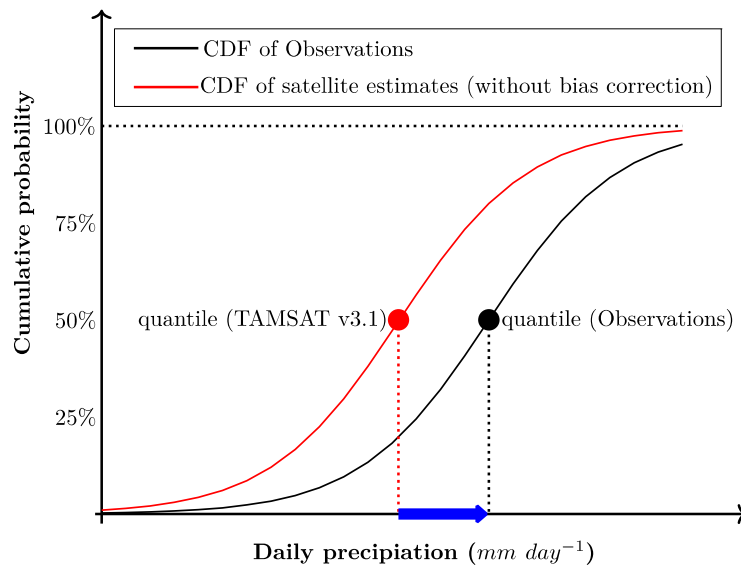


Figure 3. Schematic of the quantile mapping method, with a blue arrow highlighting the quantile-based systematic bias. Adapted from [46].

Time–space variable (TSV) bias correction addresses bias at the pixel level (i.e., variable in space) and on a daily scale (i.e., variable in time). It relies on the use of the bias correction factor (Bf_{TSV}) calculated for each gauge station. In this method, it is defined as the ratio of the sum of the gauge observations to the satellite estimations. To apply a correction that considers spatial and temporal variability in the biased SPDs, the bias factor at the station locations is interpolated to the grid of the gridded data using the inverse distance weighting (IDW) method to cover the entire study area. We followed the approach of [51] in the same study area, which showed good interpolation results using IDW. The adjusted SPDs are generated by multiplying the entire domain of raw SPDs by this correction factor value interpolated for the respective time windows [52].

When working with daily data, a fixed time window is chosen to account for temporal variability in the bias factor. A time window of either 7 or 10 days is recommended to allow sufficient accumulation of precipitation for bias calculation and to minimize discrepancies between satellite and in situ precipitation estimates [44]. In this study, a centered time window of 10 days has been implemented. Additionally, bias correction factors are calculated using only wet days with cumulative precipitation greater than or equal to 1 mm. In cases where both the gauge and satellite have zero values for a given day, correction is not applied, and the satellite estimates are set to 0 mm [10]. The equation for the multiplicative daily bias factor at a gauge location ($Bf_{TSV_{s,j}}$) is expressed as follows in Equation (3):

$$Bf_{TSV_{s,j}} = \frac{\sum_{y=1}^N \left(\sum_{t=j-\lfloor w/2 \rfloor}^{j+\lfloor w/2 \rfloor} G_{s,t,y} \right)}{\sum_{y=1}^N \left(\sum_{t=j-\lfloor w/2 \rfloor}^{j+\lfloor w/2 \rfloor} S_{s,t,y} \right)} \tag{3}$$

where $Bf_{TSV_{s,j}}$ is the bias factor for day j at a station s , $y \in [1, N]$ represents the year index from 1 to N (total number of years over the considered period), w is the centered time window size, $G_{s,t,y}$ is the gauge observation at station i on day j of year y , and $S_{s,t,y}$ is the satellite estimation at station i on day j of year y .

2.4.3. Merging Based on Regression Kriging

Regression Kriging (RK) is a hybrid spatial prediction technique that combines a deterministic model (i.e., a simple or multiple linear regression model) with a statistical

model (i.e., ordinary Kriging) of prediction residuals [23,24]. The regression component addresses systematic biases in satellite estimates, while the Kriging component accounts for local spatial variations. In this process of merging satellite and precipitation data, the first step involves establishing a deterministic relationship between gauge measurements and satellite estimates at gauge locations. This is accomplished through a linear regression model (Equation (4)). The established regression relationship is then applied to satellite data at ungauged locations s_0 to obtain initial precipitation estimates (Equation (5)). This step provides a first-order correction of satellite estimates based on their relationship with gauge measurements. Next, the residuals at gauge locations are calculated, and ordinary Kriging is applied to interpolate these residuals to ungauged locations. Finally, the merged precipitation estimate at any location is the combination of residuals at gauge locations and the first-order correction of satellite estimates [23,25,26,39]. The merged precipitation equation is presented in Equation (6):

$$pcp_{gauge}(s_i) = \beta_0 + \beta_1 pcp_{sat}(s_i) + \varepsilon(s_i) \tag{4}$$

$$\widehat{pcp}_{reg}(s_0) = \beta_0 + \beta_1 pcp_{sat}(s_0) \tag{5}$$

$$pcp_{merged}(s_0) = \underbrace{[\beta_0 + \beta_1 pcp_{sat}(s_0)]}_{\text{Regression with satellite data}} + \underbrace{\sum 1i = 1^n \lambda_i(s_0) \cdot [pcp_{gauge}(s_i) - (\beta_0 + \beta_1 pcp_{sat}(s_i))]}_{\text{Kriged residuals between gauge and satellite}} \tag{6}$$

where $pcp_{gauge}(s_i)$ represents gauge measurements at the location of gauge station s_i , $pcp_{sat}(s_i)$ represents satellite estimates at gauge locations, β_0, β_1 are regression coefficients, $\varepsilon(s_i)$ represents the regression residuals, and $pcp_{reg}(s_0)$ represents the predicted precipitation value at an unsampled location s_0

2.4.4. Evaluation Metrics

Two evaluations were conducted as part of this study. The first evaluation focuses on the validation of bias correction algorithms. Bias-corrected data (gridded data) are extracted at the rain gauge location and compared with the station data. In the second evaluation, data fusion results are extracted and compared with both bias-corrected data and station data. The comparisons involved using statistical measures such as mean error (ME), mean absolute error (MAE), root-mean-square error (RMSE), bias, and the coefficient of determination (R^2) (Table 1). For more details on the chosen measures, see [35]. In addition, some categorical statistics, including the probability of detection (POD) and false alarm ratio (FAR), are derived from the daily evaluations [35]. These categorical statistics (POD and FAR) play a crucial role in the daily evaluations, complementing the standard statistical measures (ME, MAE, RMSE, bias, and R^2) to provide a comprehensive assessment of the bias correction and the data merging. The POD indicates how effectively the system can detect actual precipitation events, while the FAR represents the proportion of false detections relative to the total number of predicted events. These metrics enable a thorough validation of both the bias correction algorithms and the data merging outcomes.

Table 1. Statistical measure for evaluation.

| Statistical Metrics | Equation | Optimum Value |
|------------------------|---|---------------|
| Root-mean-square error | $RMSE = \sqrt{\left(\frac{1}{N} \sum_{i=1}^N (S_i - G_i)^2\right)}$ | 0 |
| Mean absolute error | $MAE = \frac{1}{N} \sum_{i=1}^N G_i - S_i $ | 0 |
| Pearson’s correlation | $r = \frac{\sum_{i=1}^N (G_i - \bar{G})(S_i - \bar{S})}{\sqrt{\sum_{i=1}^N (G_i - \bar{G})^2} \sqrt{\sum_{i=1}^N (S_i - \bar{S})^2}}$ | 0 |

Table 1. *Cont.*

| Statistical Metrics | Equation | Optimum Value |
|--------------------------------|---|---------------|
| Bias | $\text{Bias} = \frac{\sum_{i=1}^N (S_i)}{\sum_{i=1}^N (G_i)}$ | 1 |
| Probability of Detection (POD) | $\text{POD} = \frac{H}{H+M}$ | 1 |
| The False Alarm Ratio (FAR) | $\text{FAR} = \frac{F}{H+F}$ | 0 |

where G_i is the gauge precipitation measurement (in mm); \bar{G} is the average gauge precipitation measurement (in mm); S_i is the satellite precipitation estimate (in mm); \bar{S} is average satellite precipitation estimate (in mm). H is the number of hits; F is the number of false alarms; and M is the number of misses.

3. Results

3.1. Quality Control Results

From an initial network of 140 rain gauges distributed across Burkina Faso (Figure 4a), quality control procedures eliminated 43 stations (31% of the original network), resulting in 97 stations with reliable records for the period of 1991–2020 (Figure 4b). These retained stations demonstrate high data quality, with the majority achieving 98–100% completeness in their daily precipitation records. The quality control assessment reveals no distinct geographical patterns in data reliability, as stations with varying levels of completeness (95–100%) are dispersed throughout the country. While the quality-controlled network maintains adequate spatial coverage for most of the country, there are notable spatial disparities: the central region (around 2° W) shows a higher density of stations, whereas the eastern region (0° to 2° E) exhibits significantly sparse coverage.

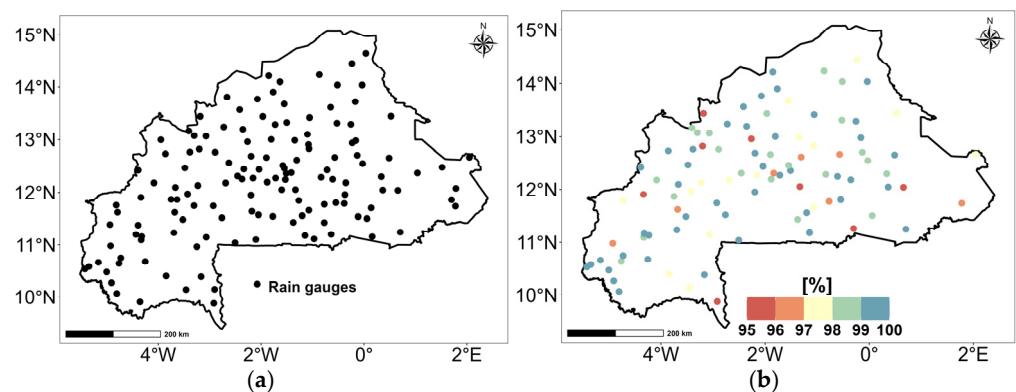


Figure 4. Spatial distribution of rain gauge stations across Burkina Faso (a) and percentage of data completeness at quality-controlled stations for the period 1991–2020 (b). The color scale indicates the percentage of available daily precipitation records at each station.

3.2. Bias Correction of TAMSAT Daily Precipitation

EQM and TSV are the two methods applied to remove the bias from TAMSAT V3.1 daily datasets. Datasets were compared before and after bias correction with the observations to identify the most effective bias correction method, specifically the one that best reduces the systematic errors in the SPDs for the study area. Validation used statistical indicators such as the root-mean-square error (RMSE), mean error (ME), bias, coefficient of determination (R^2), probability of detection (POD), and false alarm ratio (FAR) to assess the difference in accuracy between EQM and TSV bias correction methods. These results are presented in Table 2. The best values of each of these statistics are highlighted in bold. These metrics show that the quality of the two bias-corrected datasets improved compared to the uncorrected dataset. However, EQM outperformed TSV on all metrics except FAR. Indeed, the results revealed that EQM reached a much better R^2 , with a value of 0.76 against 0.55 for TSV. It also showed superior performance in terms of ME, bias, RMSE, and POD.

However, its FAR value of 0.59 was slightly higher than that of TSV (0.58), meaning that TSV was slightly more reliable in predicting true positives than EQM.

Table 2. Comparison of bias correction methods using summary statistics against the observed data.

| Metrics | TAMSAT Uncorrected | EQM | TSV | EQM Improvement (%) | TSV Improvement (%) |
|----------------|--------------------|-------|-------|---------------------|---------------------|
| R ² | 0.53 | 0.76 | 0.55 | 19.40 | 1.00 |
| Bias | 0.88 | 0.97 | 0.93 | 10.30 | 5.70 |
| ME | −0.30 | −0.08 | −0.17 | 72.30 | 43.3 |
| RMSE | 26.49 | 25.71 | 26.49 | 3.00 | 0.03 |
| POD | 0.85 | 0.86 | 0.85 | 1.30 | 0.10 |
| FAR | 0.60 | 0.59 | 0.58 | 2.30 | 3.60 |

Overall, while TAMSAT underestimated the extreme daily precipitation (Figure 5a), TSV (Figure 5b) and EQM (Figure 5c) showed a better capture of the annual cycle of the average daily precipitation. Moreover, among the two bias correction methods, EQM performed better in capturing the local maximum of the annual cycle of precipitation, which occurs at the end of the wet season.

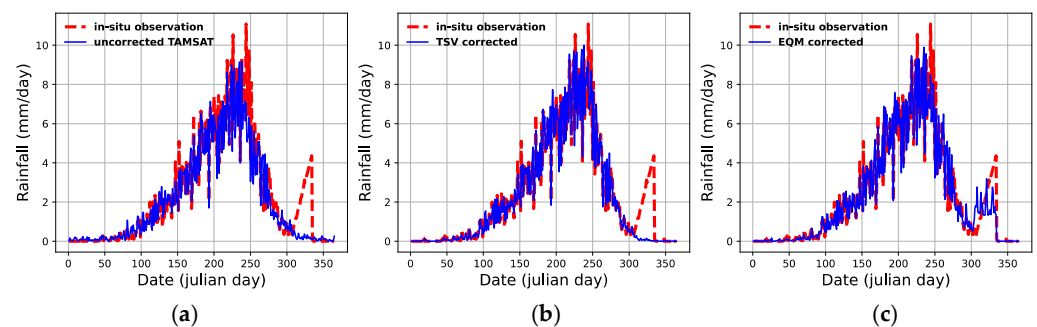


Figure 5. Comparison of average daily precipitation between TAMSAT corrected by TSV (b) and EQM (c) with reference from in situ observations (a).

The Taylor diagram presented in Figure 6 combines several key statistical measures into a single, interpretable figure and offers a comprehensive visualization of how effectively the two bias correction methods perform when applied to the original TAMSAT dataset. The diagram displays three statistics: the root-mean-square error (RMSE), the correlation coefficient (R), and the standard deviation (SD). The results show that both correction methods are valid choices for improving TAMSAT estimates; however, the EQM method considerably enhanced the uncorrected dataset. The EQM point is closer to the reference point, indicating that EQM achieved a higher correlation (greater than 0.85), appropriate SD (closer to 1), and lower centered RMSE (approximately 0.5 mm/day) than TSV for the considered period.

When considering the wet season from May to October, Figure 7 demonstrates that both bias correction methods successfully improve the TAMSAT rainfall estimates, bringing them closer to reference values. Both methods achieve similar RMS error reduction with higher correlation (approximately 0.8–0.9) and a normalized standard deviation closer to 1. However, EQM generally demonstrates more robust and consistent performance, particularly in correlation and RMS error reduction. While TSV provides effective bias correction, it shows more temporal variability in its performance. The superiority of EQM is most evident in the months of June, September, and October.

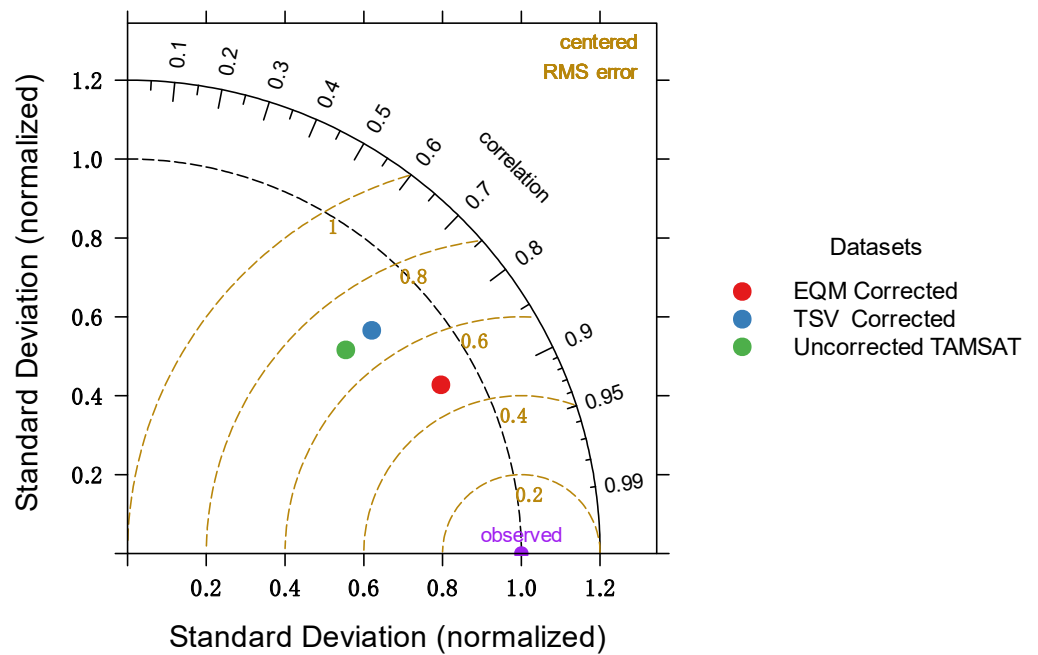


Figure 6. Taylor diagram illustrating the statistics of inter-comparison between three datasets: uncorrected, TSV corrected and EQM corrected for the period of 1991–2020.

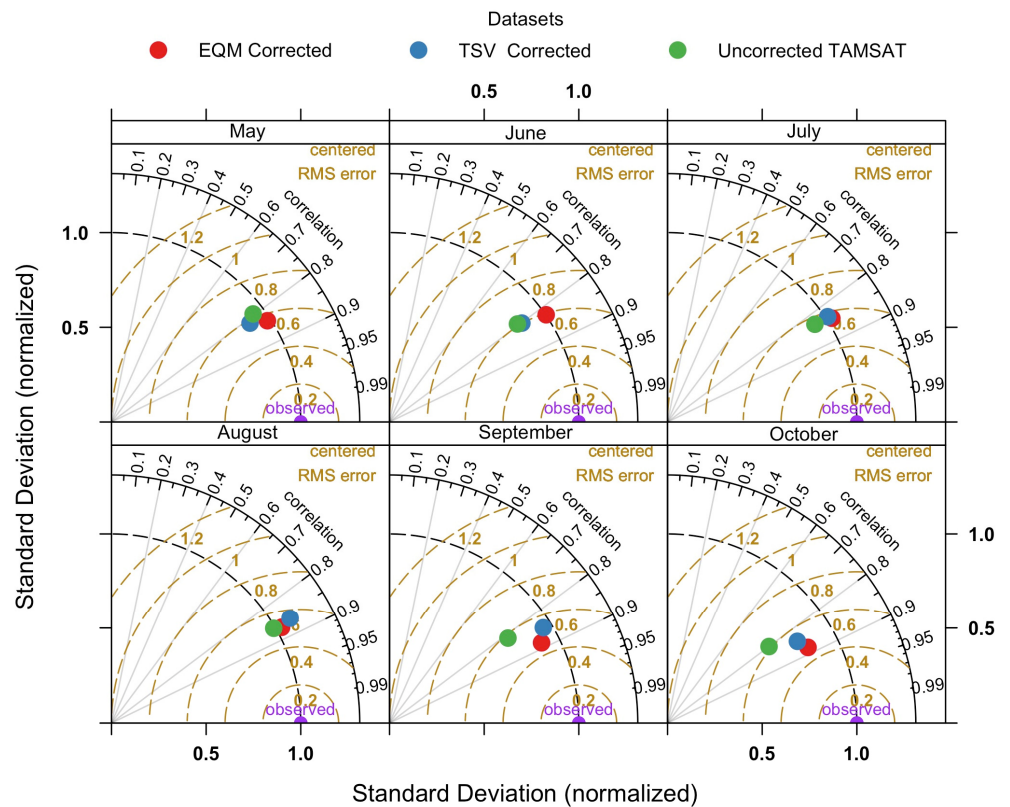


Figure 7. Taylor diagram illustrating the statistics of inter-comparison between three precipitation datasets at a monthly scale for the wet season.

3.3. Bias Correction of Extreme Daily Precipitation

The evaluation of bias correction for extreme precipitation values, covering the period from 1991 to 2020, was conducted to assess not only the overall effectiveness of the models in correcting these extreme values but also to identify the most effective correction method.

Extreme values refer to high quantiles (threshold set to the 90th percentile) of a statistical distribution from observations. Based on the rainy events over the considered period, 512 recorded precipitation events were found to be above the 90th percentile. The statistics presented in Table 3 show that the two bias correction methods significantly reduced the biases of extreme precipitation. However, the most effective bias correction method was EQM, as it significantly enhanced the R^2 , ME, RMSE, and bias. The comparison between datasets corrected by EQM and TSV, based on the annual cycle of the occurrence and value of the extreme precipitation, is illustrated in Figure 8. It was observed that, among the two methods, the TSV method did not efficiently capture the extreme values in the time series of the extreme precipitation.

Table 3. Comparison of bias correction methods in adjusting extreme precipitation.

| Metrics | TAMSAT Uncorrected | EQM | TSV | EQM Improvement (%) | TSV Improvement (%) |
|---------|--------------------|--------|--------|---------------------|---------------------|
| R^2 | 0.004 | 0.406 | 0.002 | >100 | 50 |
| Bias | 0.726 | 0.883 | 0.808 | 26.63 | 11.3 |
| ME | −3.710 | −1.580 | −2.597 | 57.41 | 30.0 |
| RMSE | 9.521 | 6.011 | 9.443 | 36.87 | 0.81 |

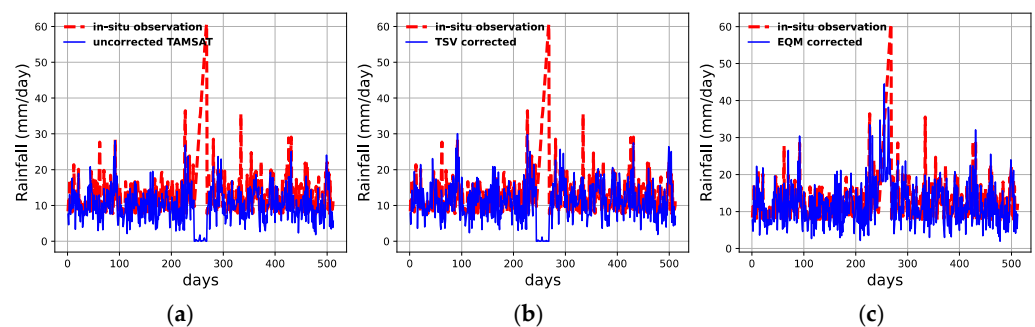


Figure 8. Comparison of extreme daily precipitation between TAMSAT corrected by TSV (b) and EQM (c) with reference from in situ observations (a).

3.4. Merging of Bias-Corrected and In Situ Observation Datasets

The Regression Kriging (RK) method was applied to the bias-corrected datasets obtained by EQM. Table 4 summarizes the results of the statistical analysis. The analysis showed that the merged dataset was more accurate than the bias-corrected dataset by all measures, as the coefficient of determination and bias were about 0.97 and 0.98, respectively. The bias-corrected dataset had the largest ME in absolute value and a much larger RMSE than the merged dataset. With a POD of 0.99 compared to 0.86 for the bias-corrected dataset, the merged dataset detected precipitation events better with a lower false alarm rate (FAR = 0.01). The RK merging approach improved the correlation by 83%, the bias by 11.4%, the mean error by 96.7%, and the RMSE by 95.5%.

Figure 9 provides an overview of the improvement made by merging the bias-corrected datasets with the rain gauge data. In Figure 9a, the unmerged dataset corrected by EQM showed underestimations of the daily precipitation for rainy events with the lowest or highest precipitation measurements. After the merging was performed (Figure 9b), a significant improvement was observed. The merged and in situ datasets showed a more accurate match, indicating that the merged dataset fully captured the annual cycle of the daily precipitation.

Table 4. Statistics on daily merged precipitation.

| Metrics | TAMSAT Uncorrected | Bias Corrected (Unmerged) | Merged Dataset | Final Improvements (%) |
|----------------|--------------------|---------------------------|----------------|------------------------|
| R ² | 0.53 | 0.76 | 0.97 | 83.02 |
| Bias | 0.88 | 0.97 | 0.98 | 11.36 |
| ME | −0.30 | −0.08 | 0.01 | 96.67 |
| RMSE | 26.49 | 25.71 | 1.18 | 95.54 |
| POD | 0.85 | 0.86 | 0.99 | 16.47 |
| FAR | 0.60 | 0.59 | 0.01 | 98.33 |

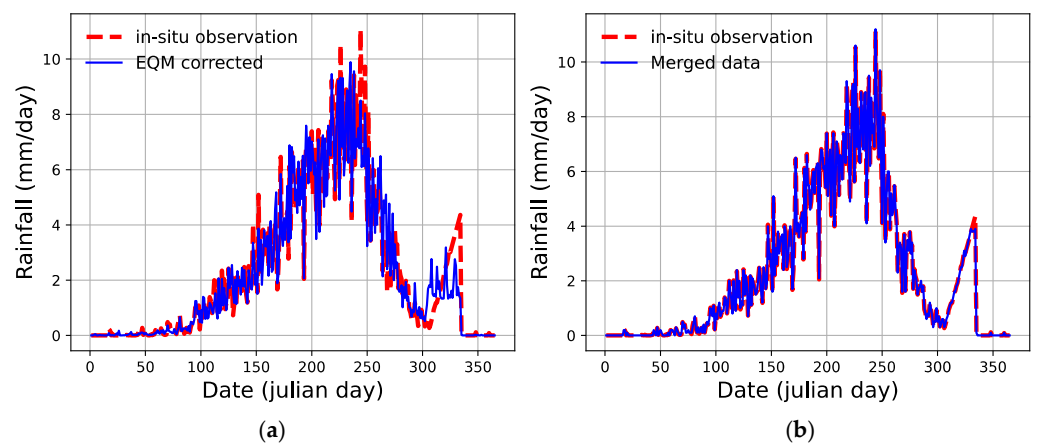


Figure 9. Average daily precipitation from TAMSAT satellite data corrected using (a) EQM method and (b) merging the bias-corrected datasets with rain gauge data using the merging approach, both compared with ground-based observations.

3.5. Spatial Distribution of Merging of Bias-Corrected and In Situ Observation Datasets

Merging precipitation products are analyzed to examine the merge method's ability to effectively combine two databases over three key periods, i.e., early season, mid-season, and late season. As a case study, Figure 10 depicts the precipitation pattern for 7 May 2010 (Figure 10a–c), 29 July 2010 (Figure 10d–f), and 6 October 2010 (Figure 10g–i), corresponding to three rainy events during the early season, mid-season, and late season in 2010, respectively. Overall, when in situ observations are merged with TAMSAT estimates (Figure 10c,f,i), the spatial distribution of precipitation is well captured, regardless of the considered periods. However, we observed that while the location of rainy events from in situ observations in the early and mid-seasons (Figure 10a,c) is well captured by satellite estimates (Figure 10b,h), the precipitation amount is underestimated in some locations. Among the three considered dates, TAMSAT estimates performed better on the mid-season date, but this performance is still lower than that of the merged dataset.

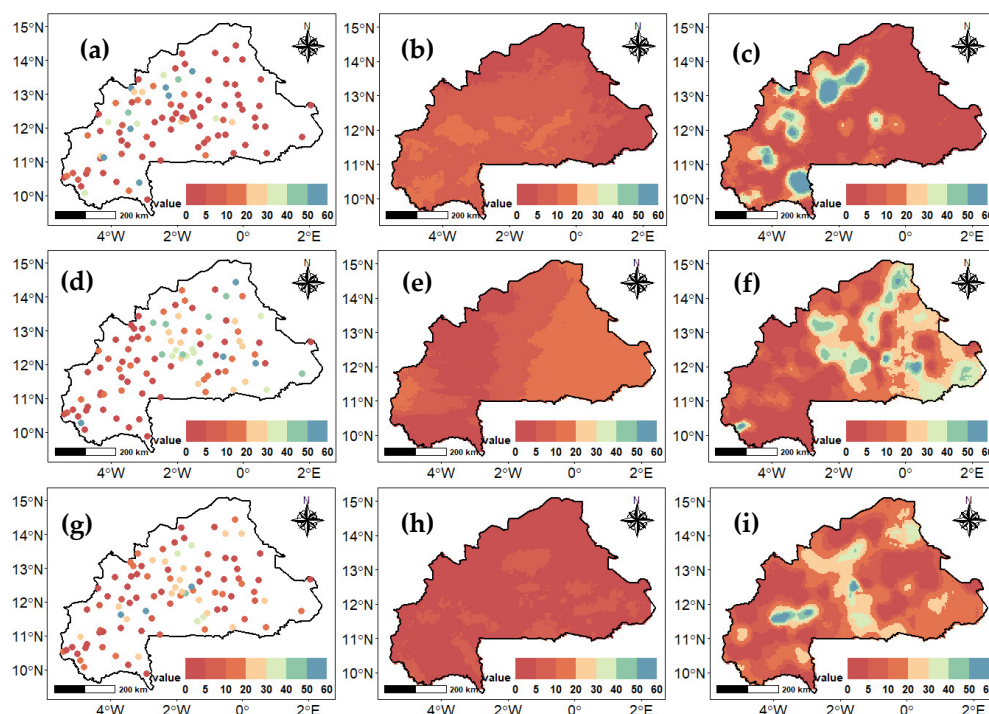


Figure 10. The spatial distribution of the merging for rainy events on 7 May 2010 (**top**), 29 July 2010 (**middle**), and 6 October 2010 (**bottom**). These three periods correspond to the early season, mid-season, and the end season of the wet season, respectively. Dataset sources are station observations (**a,d,g**), original TAMSAT data (**b,e,h**), and merged products (**c,f,i**).

4. Discussion

This paper focuses on enhancing the accuracy of satellite-derived precipitation data through bias correction and merging techniques, using Burkina Faso as a case study. This region is critical for agriculture and water resource management due to its semi-arid conditions and reliance on the rainy season [30,53]. Overall, it addresses a significant challenge in meteorological and agricultural research: the crucial role of rainfall in agricultural productivity, water resource management, and food security in the semi-arid Sahel region [53,54]. It also highlights the potential to improve capabilities for monitoring and managing climate-related risks, such as droughts and floods. By examining the efficacy of bias correction and merging techniques across Burkina Faso, this research aligns with the scientific community's efforts to address the limitations posed by sparse and uneven distributions of ground-based observation networks [33]. The study's approach of first applying bias correction techniques to SPDs before merging them with ground-based data represents a methodological advancement.

The application of bias correction techniques, notably Empirical Quantile Mapping (EQM) and Time and Space Variant (TSV), demonstrates the importance of correcting systematic errors in satellite precipitation datasets (SPDs). The results indicate that EQM outperforms TSV in key statistical metrics such as R^2 , ME, RMSE, and POD, except for the FAR. This outcome aligns with previous studies that highlight the superior performance of distribution-based approaches over linear and non-linear methods in accurately capturing precipitation patterns [16,19]. These results reinforce the argument that EQM, despite its straightforward approach, effectively addresses the biases inherent in satellite-derived precipitation estimates, making it a powerful tool for improving the quality of SPDs.

Rainfall data from gauges are point measurements, unlike satellite remote sensing data, which provide a spatial distribution of precipitation. Therefore, merging is essentially a method that leverages the strengths and mitigates the weaknesses of both remote sensing and rain gauges, resulting in better outcomes than using either method alone, as shown in

this study and confirmed by other studies [21,22]. This study highlights the considerable added value of merging bias-corrected SPDs with rain gauge data. While some studies have focused solely on bias correction [43,50] and others on directly merging in situ data and satellite data [40,55], the proposed dual approach not only enhances spatial coverage but also improves the temporal consistency of the resultant dataset, thus more accurately reflecting local precipitation patterns. These outcomes corroborate the advantages of merged approaches as documented in the previous literature, particularly concerning the integration of both spatial and temporal measurements [21,22]. Consequently, it has led to the widespread adoption of merging techniques in various regions, including India [56], South Korea [57], China [58], America [59], Europe [60], and Africa through the Enhancing National Climate Services (ENACTSs) [33].

With the Sahel's agriculture and water resource management highly dependent on rainfall, the ability to provide accurate, high-resolution precipitation data is crucial. From a broader perspective, improved SPD accuracy can significantly support the validation of climate models and anticipate and mitigate the adverse impacts of weather conditions in agriculture and water resources through enhanced agricultural decision-making. For instance, enhanced precipitation data are vital for activities such as crop planning, irrigation scheduling, water allocation and conservation, and developing and implementing adaptation strategies [3,5,61].

Despite the added value of the proposed merging approach, certain limitations must be acknowledged. The accuracy of the merged dataset is influenced by the density and distribution of rain gauges, which can vary regionally [19]. Additionally, while EQM and TSV have shown effectiveness in bias correction, the search for a robust method is still ongoing. As a perspective, future research could explore the integration of additional data sources, such as radar or reanalysis data, to further refine precipitation estimates. Incorporating radar data might provide high-resolution spatial and temporal information, which can be particularly valuable in capturing localized rainfall events that rain gauges might miss [38]. Moreover, extending the study to other regions with different climatic conditions could contribute to validating the robustness of the proposed method, thereby supporting climate research and resource management strategies in varied climatic zones.

5. Conclusions

In conclusion, we have proposed an approach that combines rain gauge observations with satellite precipitation estimates on a daily time step to improve the accuracy of precipitation data. This methodology involves the quality control of rain gauge observations, bias correction of the TAMSAT dataset, and the implementation of the Regression Kriging technique to merge the best bias-corrected dataset with rain gauge observations. The performance of the merged precipitation data has been statistically evaluated through comparisons with historic rain gauge datasets. The results indicate that EQM outperforms TSV in key statistical metrics, and the analysis of the merged precipitation data underscores the considerable added value of integrating bias-corrected SPDs with rain gauge data. Therefore, the proposed dual approach not only enhances spatial coverage but also improves the temporal consistency of the resultant dataset, thereby more accurately reflecting local precipitation patterns. The operational implementation of this approach provides substantial support for decision-making in regions heavily reliant on rainfed agriculture and sensitive to climate variability. By yielding more precise and reliable precipitation datasets, it enables more informed decisions and significantly enhances policy-making processes in the agricultural and water resources sectors of Burkina Faso.

Author Contributions: Conceptualization, M.W.; Methodology, M.W. and J.N.G.; Software, J.N.G.; Formal analysis, M.W., J.N.G. and U.J.D.; Investigation, J.N.G.; Data curation, J.N.G. and W.L.S.; Writing—original draft, M.W. and J.N.G.; Writing—review & editing, U.J.D. and W.S.; Supervision, T.D.; Project administration, M.W. All authors have read and agreed to the published version of the manuscript.

Funding: This work was funded by the German Federal Ministry of Education and Research (BMBF) research project CONCERT (grant number 01LG2101A) through the West African Science Center for Climate Change and Adapted Land Use (WASCAL)

Data Availability Statement: The observed precipitation data from the National Meteorological Agency of Burkina Faso (ANAM-BF) mentioned in this article are not readily available due to national data access policies. Requests for access to these datasets should be directed to the National Meteorological Agency of Burkina Faso at meteoburkina@yahoo.fr.

Acknowledgments: We would like to thank the National Meteorological Agency of Burkina Faso (ANAM-BF) for providing daily precipitation data from 140 rain gauges in their weather observation network. We also acknowledge the anonymous reviewers for their valuable comments.

Conflicts of Interest: The authors declare no conflicts of interest.

References

1. Biasutti, M. Rainfall Trends in the African Sahel: Characteristics, Processes, and Causes. *WIREs Clim. Chang.* **2019**, *10*, e591. [[CrossRef](#)]
2. Tsowa, U.M.; Abdulkadir, A. Livelihoods Sustainability in Agriculture-Intensive Semi-Arid and Dry Sub-Humid Areas of West Africa—Pointers from Nigeria 2019. *Preprints* **2019**, 2019010234. [[CrossRef](#)]
3. Sultan, B.; Gaetani, M. Agriculture in West Africa in the Twenty-First Century: Climate Change and Impacts Scenarios, and Potential for Adaptation. *Front. Plant Sci.* **2016**, *7*, 1262. [[CrossRef](#)]
4. Trisos, C.; Adelekan, I.; Totin, E.; Ayanlade, A.; Efitre, J.; Gemedda, A.; Kalaba, K.; Lennard, C.; Masao, C.; Mgya, Y.; et al. *Climate Change 2022—Impacts, Adaptation and Vulnerability: Working Group II Contribution to the Sixth Assessment Report of the Intergovernmental Panel on Climate Change*; Intergovernmental Panel on Climate Change (IPCC), Ed.; Cambridge University Press: Cambridge, UK, 2023; pp. 1285–1456, ISBN 978-1-00-932583-7.
5. Washington, R.; Harrison, M.; Conway, D.; Black, E.; Challinor, A.; Grimes, D.; Jones, R.; Morse, A.; Kay, G.; Todd, M. African Climate Change: Taking the Shorter Route. *Bull. Am. Meteorol. Soc.* **2006**, *87*, 1355–1366. [[CrossRef](#)]
6. Tang, L.; Tian, Y.; Yan, F.; Habib, E. An Improved Procedure for the Validation of Satellite-Based Precipitation Estimates. *Atmos. Res.* **2015**, *163*, 61–73. [[CrossRef](#)]
7. Sadeghi, M.; Asanjan, A.A.; Faridzad, M.; Nguyen, P.; Hsu, K.; Sorooshian, S.; Braithwaite, D. PERSIANN-CNN: Precipitation Estimation from Remotely Sensed Information Using Artificial Neural Networks—Convolutional Neural Networks. *J. Hydrometeorol.* **2019**, *20*, 2273–2289. [[CrossRef](#)]
8. Smith, T.M.; Arkin, P.A.; Bates, J.J.; Huffman, G.J. Estimating Bias of Satellite-Based Precipitation Estimates. *J. Hydrometeorol.* **2006**, *7*, 841–856. [[CrossRef](#)]
9. Gebremicael, T.G.; Mohamed, Y.A.; van der Zaag, P.; Berhe, A.G.; Haile, G.G.; Hagos, E.Y.; Hagos, M.K. Comparison and Validation of Eight Satellite Rainfall Products over the Rugged Topography of Tekeze-Atbara Basin at Different Spatial and Temporal Scales. *Hydrol. Earth Syst. Sci. Discuss.* **2017**, *2017*, 1–31. [[CrossRef](#)]
10. Gumindoga, W.; Rientjes, T.H.M.; Haile, A.T.; Makurira, H.; Reggiani, P. Performance of Bias-Correction Schemes for CMORPH Rainfall Estimates in the Zambezi River Basin. *Hydrol. Earth Syst. Sci.* **2019**, *23*, 2915–2938. [[CrossRef](#)]
11. Jakob Themeßl, M.; Gobiet, A.; Leuprecht, A. Empirical-statistical Downscaling and Error Correction of Daily Precipitation from Regional Climate Models. *Int. J. Climatol.* **2011**, *31*, 1530–1544. [[CrossRef](#)]
12. Teutschbein, C.; Seibert, J. Bias Correction of Regional Climate Model Simulations for Hydrological Climate-Change Impact Studies: Review and Evaluation of Different Methods. *J. Hydrol.* **2012**, *456–457*, 12–29. [[CrossRef](#)]
13. Chen, J.; Brissette, F.P.; Chaumont, D.; Braun, M. Finding Appropriate Bias Correction Methods in Downscaling Precipitation for Hydrologic Impact Studies over North America. *Water Resour. Res.* **2013**, *49*, 4187–4205. [[CrossRef](#)]
14. Lafon, T.; Dadson, S.; Buys, G.; Prudhomme, C. Bias Correction of Daily Precipitation Simulated by a Regional Climate Model: A Comparison of Methods. *Int. J. Climatol.* **2013**, *33*, 1367–1381. [[CrossRef](#)]
15. Chen, J.; St-Denis, B.G.; Brissette, F.P.; Lucas-Picher, P. Using Natural Variability as a Baseline to Evaluate the Performance of Bias Correction Methods in Hydrological Climate Change Impact Studies. *J. Hydrometeorol.* **2016**, *17*, 2155–2174. [[CrossRef](#)]
16. Goshime, D. Integration of Satellite and Ground-Based Rainfall Data for Water Resources Assessment in Central Rift Valley Lakes Basin, Ethiopia. Ph.D. Thesis, CY Cergy Paris Université, Cergy, France, 2020.
17. Choudhary, A.; Dimri, A.P. On Bias Correction of Summer Monsoon Precipitation over India from CORDEX-SA Simulations. *Int. J. Climatol.* **2019**, *39*, 1388–1403. [[CrossRef](#)]
18. Ehret, U.; Zehe, E.; Wulfmeyer, V.; Warrach-Sagi, K.; Liebert, J. HESS Opinions “Should We Apply Bias Correction to Global and Regional Climate Model Data”? *Hydrol. Earth Syst. Sci.* **2012**, *16*, 3391–3404. [[CrossRef](#)]
19. Lakew, H.B. Investigating the Effectiveness of Bias Correction and Merging MSWEP with Gauged Rainfall for the Hydrological Simulation of the Upper Blue Nile Basin. *J. Hydrol. Reg. Stud.* **2020**, *32*, 100741. [[CrossRef](#)]
20. Datta, S.; Jones, W.L.; Roy, B.; Tokay, A. Spatial Variability of Surface Rainfall as Observed from TRMM Field Campaign Data. *J. Appl. Meteorol. Clim.* **2003**, *42*, 598–610. [[CrossRef](#)]

21. Duque-Gardeazabal, N.; Zamora, D.; Rodriguez, E. Analysis of the Kernel Bandwidth Influence in the Double Smoothing Merging Algorithm to Improve Rainfall Fields in Poorly Gauged Basins. In Proceedings of the 13th International Conference on Hydroinformatics (HIC 2018), Palermo, Italy, 1–6 July 2018.
22. Bhuiyan, M.A.E.; Nikolopoulos, E.I.; Anagnostou, E.N. Machine Learning–Based Blending of Satellite and Reanalysis Precipitation Datasets: A Multiregional Tropical Complex Terrain Evaluation. *J. Hydrometeorol.* **2019**, *20*, 2147–2161. [[CrossRef](#)]
23. Odeh, I.O.A.; McBratney, A.B.; Chittleborough, D.J. Further Results on Prediction of Soil Properties from Terrain Attributes: Heterotopic Cokriging and Regression-Kriging. *Geoderma* **1995**, *67*, 215–226. [[CrossRef](#)]
24. Goovaerts, P. *Geostatistics for Natural Resources Evaluation*; Oxford University Press: Oxford, UK, 1997; ISBN 978-0-19-511538-3.
25. Hengl, T.; Heuvelink, G.B.M.; Rossiter, D.G. About Regression-Kriging: From Equations to Case Studies. *Comput. Geosci.* **2007**, *33*, 1301–1315. [[CrossRef](#)]
26. Gia Pham, T.; Kappas, M.; Van Huynh, C.; Hoang Khanh Nguyen, L. Application of Ordinary Kriging and Regression Kriging Method for Soil Properties Mapping in Hilly Region of Central Vietnam. *ISPRS Int. J. Geo-Inf.* **2019**, *8*, 147. [[CrossRef](#)]
27. Beck, H.E.; Van Dijk, A.I.; Levizzani, V.; Schellekens, J.; Miralles, D.G.; Martens, B.; De Roo, A. MSWEP: 3-hourly 0.25 Global Gridded Precipitation (1979–2015) by Merging Gauge, Satellite, and Reanalysis Data. *Hydrol. Earth Syst. Sci.* **2017**, *21*, 589–615. [[CrossRef](#)]
28. Kidd, C.; Becker, A.; Huffman, G.J.; Muller, C.L.; Joe, P.; Skofronick-Jackson, G.; Kirschbaum, D.B. So, How Much of the Earth’s Surface Is Covered by Rain Gauges? *Bull. Am. Meteorol. Soc.* **2017**, *98*, 69–78. [[CrossRef](#)]
29. Huffman, G.J.; Adler, R.F.; Bolvin, D.T.; Gu, G. Improving the Global Precipitation Record: GPCP Version 2.1. *Geophys. Res. Lett.* **2009**, *36*, L17808. [[CrossRef](#)]
30. Sivakumar, M.V.K.; Gnoumou, F. Agroclimatology of West Africa: Burkina Faso. Available online: <https://oar.icrisat.org/864/> (accessed on 5 August 2024).
31. Oueslati, B.; Camberlin, P.; Zoungrana, J.; Roucou, P.; Diallo, S. Variability and Trends of Wet Season Temperature in the Sudano-Sahelian Zone and Relationships with Precipitation. *Clim. Dyn.* **2018**, *50*, 1067–1090. [[CrossRef](#)]
32. Tirogo, J.; Jost, A.; Biaou, A.; Valdes-Lao, D.; Koussoubé, Y.; Ribstein, P. Climate Variability and Groundwater Response: A Case Study in Burkina Faso (West Africa). *Water* **2016**, *8*, 171. [[CrossRef](#)]
33. Dinku, T. Challenges with Availability and Quality of Climate Data in Africa. In *Extreme Hydrology and Climate Variability*; Melesse, A.M., Abtew, W., Senay, G., Eds.; Elsevier: Amsterdam, The Netherlands, 2019; Chapter 7; pp. 71–80, ISBN 978-0-12-815998-9.
34. Maidment, R.I.; Grimes, D.; Black, E.; Tarnavsky, E.; Young, M.; Greatrex, H.; Allan, R.P.; Stein, T.; Nkonde, E.; Senkunda, S.; et al. A New, Long-Term Daily Satellite-Based Rainfall Dataset for Operational Monitoring in Africa. *Sci. Data* **2017**, *4*, 170063. [[CrossRef](#)] [[PubMed](#)]
35. Garba, J.N.; Diasso, U.J.; Waongo, M.; Sawadogo, W.; Daho, T. Performance Evaluation of Satellite-Based Rainfall Estimation across Climatic Zones in Burkina Faso. *Theor. Appl. Clim.* **2023**, *154*, 1051–1073. [[CrossRef](#)]
36. Wang, F. WMO Information System: Beijing Global Information System Center. *Bull. Am. Meteorol. Soc.* **2013**, *94*, 991–994. [[CrossRef](#)]
37. Feng, S.; Hu, Q.; Qian, W. Quality Control of Daily Meteorological Data in China, 1951–2000: A New Dataset. *Int. J. Climatol.* **2004**, *24*, 853–870. [[CrossRef](#)]
38. Ochoa-Rodriguez, S.; Wang, L.-P.; Willems, P.; Onof, C. A Review of Radar-Rain Gauge Data Merging Methods and Their Potential for Urban Hydrological Applications. *Water Resour. Res.* **2019**, *55*, 6356–6391. [[CrossRef](#)]
39. De Vera, A.; Alfaro, P.; Terra, R. Operational Implementation of Satellite-Rain Gauge Data Merging for Hydrological Modeling. *Water* **2021**, *13*, 533. [[CrossRef](#)]
40. Atiah, W.A.; Amekudzi, L.K.; Aryee, J.N.A.; Preko, K.; Danuor, S.K. Validation of Satellite and Merged Rainfall Data over Ghana, West Africa. *Atmosphere* **2020**, *11*, 859. [[CrossRef](#)]
41. Ogbu, K.N.; Houngoué, N.R.; Gbode, I.E.; Tischbein, B. Performance Evaluation of Satellite-Based Rainfall Products over Nigeria. *Climate* **2020**, *8*, 103. [[CrossRef](#)]
42. Sennikovs, J.; Bethers, U. Statistical Downscaling Method of Regional Climate Model Results for Hydrological Modelling. In Proceedings of the 18th World IMACS/MODSIM Congress, Cairns, Australia, 13–17 July 2009.
43. Luo, M.; Liu, T.; Meng, F.; Duan, Y.; Frankl, A.; Bao, A.; De Maeyer, P. Comparing Bias Correction Methods Used in Downscaling Precipitation and Temperature from Regional Climate Models: A Case Study from the Kaidu River Basin in Western China. *Water* **2018**, *10*, 1046. [[CrossRef](#)]
44. Habib, E.; Haile, A.T.; Sazib, N.; Zhang, Y.; Rientjes, T. Effect of Bias Correction of Satellite-Rainfall Estimates on Runoff Simulations at the Source of the Upper Blue Nile. *Remote Sens.* **2014**, *6*, 6688–6708. [[CrossRef](#)]
45. Gutjahr, O.; Heinemann, G. Comparing Precipitation Bias Correction Methods for High-Resolution Regional Climate Simulations Using COSMO-CLM: Effects on Extreme Values and Climate Change Signal. *Theor. Appl. Clim.* **2013**, *114*, 511–529. [[CrossRef](#)]
46. Kim, D.; Kwon, H.-H.; Lee, S.-O.; Kim, S. Regionalization of the Modified Bartlett–Lewis Rectangular Pulse Stochastic Rainfall Model across the Korean Peninsula. *J. Hydro-Environ. Res.* **2016**, *11*, 123–137. [[CrossRef](#)]
47. Ayugi, B.O.; Chung, E.-S.; Zhu, H.; Ogega, O.M.; Babousmail, H.; Ongoma, V. Projected Changes in Extreme Climate Events over Africa under 1.5 °C, 2.0 °C and 3.0 °C Global Warming Levels Based on CMIP6 Projections. *Atmos. Res.* **2023**, *292*, 106872. [[CrossRef](#)]

48. Yang, Z.; Hsu, K.; Sorooshian, S.; Xu, X.; Braithwaite, D.; Verbist, K.M.J. Bias Adjustment of Satellite-Based Precipitation Estimation Using Gauge Observations: A Case Study in Chile. *J. Geophys. Res. Atmos.* **2016**, *121*, 3790–3806. [[CrossRef](#)]
49. Wilks, D.S. *Statistical Methods in the Atmospheric Sciences*; Academic Press: Cambridge, MA, USA, 2011; ISBN 978-0-12-385023-2.
50. Piani, C.; Weedon, G.P.; Best, M.; Gomes, S.M.; Viterbo, P.; Hagemann, S.; Haerter, J.O. Statistical Bias Correction of Global Simulated Daily Precipitation and Temperature for the Application of Hydrological Models. *J. Hydrol.* **2010**, *395*, 199–215. [[CrossRef](#)]
51. Haile, A.T.; Rientjes, T.; Gieske, A.; Gebremichael, M. Rainfall Variability over Mountainous and Adjacent Lake Areas: The Case of Lake Tana Basin at the Source of the Blue Nile River. *J. Appl. Meteorol. Clim.* **2009**, *48*, 1696–1717. [[CrossRef](#)]
52. Bhatti, H.A.; Rientjes, T.; Haile, A.T.; Habib, E.; Verhoef, W. Evaluation of Bias Correction Method for Satellite-Based Rainfall Data. *Sensors* **2016**, *16*, 884. [[CrossRef](#)]
53. Lèye, B.; Zouré, C.O.; Yonaba, R.; Karambiri, H. Water Resources in the Sahel and Adaptation of Agriculture to Climate Change: Burkina Faso. In *Climate Change and Water Resources in Africa: Perspectives and Solutions Towards an Imminent Water Crisis*; Diop, S., Scheren, P., Niang, A., Eds.; Springer International Publishing: Cham, Switzerland, 2021; pp. 309–331, ISBN 978-3-030-61225-2.
54. Bilali, H.E. Climate Change and Agriculture in Burkina Faso. *J. Arid. Agric.* **2021**, *7*, 22–47. [[CrossRef](#)]
55. Verdin, A.; Funk, C.; Rajagopalan, B.; Kleiber, W. Kriging and Local Polynomial Methods for Blending Satellite-Derived and Gauge Precipitation Estimates to Support Hydrologic Early Warning Systems. *IEEE Trans. Geosci. Remote Sens.* **2016**, *54*, 2552–2562. [[CrossRef](#)]
56. Mitra, A.K.; Bohra, A.K.; Rajeevan, M.N.; Krishnamurti, T.N. Daily Indian Precipitation Analysis Formed from a Merge of Rain-Gauge Data with the TRMM TMPA Satellite-Derived Rainfall Estimates. *J. Meteorol. Soc. Jpn. Ser. II* **2009**, *87A*, 265–279. [[CrossRef](#)]
57. Kim, B.S.; Hong, J.B.; Kim, H.S.; Yoon, S.Y. Combining Radar and Rain Gauge Rainfall Estimates for Flood Forecasting Using Conditional Merging Method. In *World Environmental and Water Resources Congress 2007: Restoring Our Natural Habitat*; American Society of Civil Engineers: Reston, VA, USA, 2012; pp. 1–16. [[CrossRef](#)]
58. Xie, P.; Xiong, A.-Y. A Conceptual Model for Constructing High-Resolution Gauge-Satellite Merged Precipitation Analyses. *J. Geophys. Res. Atmos.* **2011**, *116*, D21106. [[CrossRef](#)]
59. Vila, D.A.; de Goncalves, L.G.G.; Toll, D.L.; Rozante, J.R. Statistical Evaluation of Combined Daily Gauge Observations and Rainfall Satellite Estimates over Continental South America. *J. Hydrometeorol.* **2009**, *10*, 533–543. [[CrossRef](#)]
60. Pulkkinen, S.; Koistinen, J.; Kuitunen, T. Gauge-Radar Adjustment by Using Multivariate Kernel Regression and Spatiotemporal Kriging. 2014. Available online: https://www.researchgate.net/profile/Seppo-Pulkkinen-2/publication/270100233_ERAD_extended_abstract/links/549fe5c90cf257a635fe8e0f/ERAD-extended-abstract.pdf (accessed on 12 October 2024).
61. Rockström, J.; Falkenmark, M. Agriculture: Increase Water Harvesting in Africa. *Nature* **2015**, *519*, 283–285. [[CrossRef](#)]

Disclaimer/Publisher’s Note: The statements, opinions and data contained in all publications are solely those of the individual author(s) and contributor(s) and not of MDPI and/or the editor(s). MDPI and/or the editor(s) disclaim responsibility for any injury to people or property resulting from any ideas, methods, instructions or products referred to in the content.